

Electronic Supplementary Information

Metal Ions Induced Dual Switchable Dielectric and Luminescent

Properties in Hybrid Halides

Jia Liu,^a Li-Jun Han,^a Ting Shao,^a Chang-Yuan Su,^b Ming Chen,^b Pei-Zhi Huang,^a Qiang-Qiang Jia,^a Da-Wei Fu^{*a} and Hai-Feng Lu^{*a}

a. Institute for Science and Applications of Molecular Ferroelectrics, Key Laboratory of the Ministry of Education for Advanced Catalysis Materials, Zhejiang Normal University, Jinhua, 321004, P. R. China.

*E-mail: luhaifeng@zjnu.edu.cn dawei@zjnu.edu.cn

b. Ordered Matter Science Research Centre, Jiangsu Key Laboratory for Science and Applications of Molecular Ferroelectrics, Southeast University, Nanjing 211189, P.R. China.

Experiments section

Synthesis

All reagents and solvents used in this study are commercial analytical grade resources without further purification. To get compound **1**, 3-Chloro-N,N-dimethylaniline (3mmol, 0.467 g) was dissolved in hydrochloric acid (20 mL), add 10 ml water for further dissolution, and then metal halide BiCl₃ (3mmol, 0.946 g) was added to obtain the mixed solution. The synthesis method of the other three compounds is similar to that of compound **1**, where the metal halides are replaced by ZnCl₂ (3mmol, 0.409g), CdCl₂ (3mmol, 0.685g), MnCl₂ (3mmol, 0.286g). The four mixed solutions are stirred at room temperature until completely dissolved, lately, a clear solution is obtained. Then, the slow evaporation at room temperature was carried out for about three weeks to obtain colorless prismatic crystals (compounds **1** and **2**), colorless block, and green prismatic crystals respectively.

X-ray Single Crystal Diffraction

Variable-temperature single-crystal X-ray diffraction information was collected by using Bruker APEX-II CCD with Mo K α radiation ($\lambda = 0.71073 \text{ \AA}$). Compound **1** was collected at 273 K and 320 K, compounds **2** and **3** collected at 273 K, and compound **4** was collected at 273 K, 358 K, and 365 K respectively. Data processing was finished by APEX3. The crystal structure of compounds **1** and **2** before and after phase transition were solved by direct method and refined by full-matrix least-squares methods based on F2 in the SHELXTL software package. All non-hydrogen atoms were refined

anisotropically and the positions of all hydrogen atoms were generated geometrically. The asymmetric unit and packing diagrams of compounds **1** and **2** were drawn by DIAMOND software.

Dielectric correlation measurement

DSC measurements were carried out by PerkinElmer diamond DSC instrument in nitrogen atmosphere, 9 mg powder samples of compounds **1** and **2** were weighed and placed in an aluminum crucible, and then heated and cooled at a heating rate of 20 K min⁻¹ in the temperature range of 255 K to 355 K and 335 K to 375 K, respectively. Thermogravimetric analysis (TGA) was performed on a TA Q50 system in the temperature range of 350 K to 950 K and 300 K to 1000 K with heating rate of 10 K min⁻¹.

Temperature-Dependent Dielectric Permittivity Measurements and Powder X-ray Diffractions.

The powder-pressed pellet of compounds **1** and **2** pasted with carbon conducting glue was used in dielectric measurements. The dielectric constant in heating and cooling cycles was measured on Tonghui th28a instrument.

Powder X-ray diffraction (PXRD) data for compounds **1** and **2** were measured on a D8 Advance03030502 X-ray diffractometer at room temperature. Diffraction patterns were collected in the 2 θ range of 5~55° with a step size of 0.02°.

Photoluminescence Spectrum Measurements

The solid-state excitation and emission spectra of compound **2** were measured on the Edinburgh FLS-920 fluorescence spectrometer. The absolute quantum efficiency is measured by the combined use of the Edinburgh FLS-920 fluorescence spectrometer and integrating sphere to obtain the photoluminescence quantum yield (PLQY).

Hirshfeld Surfaces and Intermolecular Interaction Analysis

Use the crystal explorer program to calculate Hirshfeld surface and two-dimensional fingerprint, compound **1** and compound **2**, and input the structure file in

CIF format under 273 K / 320 K and 273 K / 358 K / 365 K. In this work, all the Hirshfeld surfaces were generated using a standard (high) surface resolution. The 3D Hirshfeld surfaces and 2D fingerprint plots are unique for any crystal structure. The intensity of molecular interaction is mapped onto the Hirshfeld surface by using the respective red-blue-white scheme: where the red, white, and blue are represent the contacts shorter than, equal to, and longer than the van der Waals distances, respectively. In 2D fingerprint plots, each point represents an individual pair (d_i , d_e), reflecting the distances to the nearest atom inside (d_i) and outside (d_e) of the Hirshfeld d_{norm} surface.

$$d_{norm} = \frac{d_i - r^{vdW}}{r_i^{vdW}} + \frac{d_e - r}{r_e^{vdW}}$$

d_{norm} surface represents close intermolecular interactions.

For clear analysis and comparison, we focus on the selected cations with relatively stronger contacts in the respective structures.

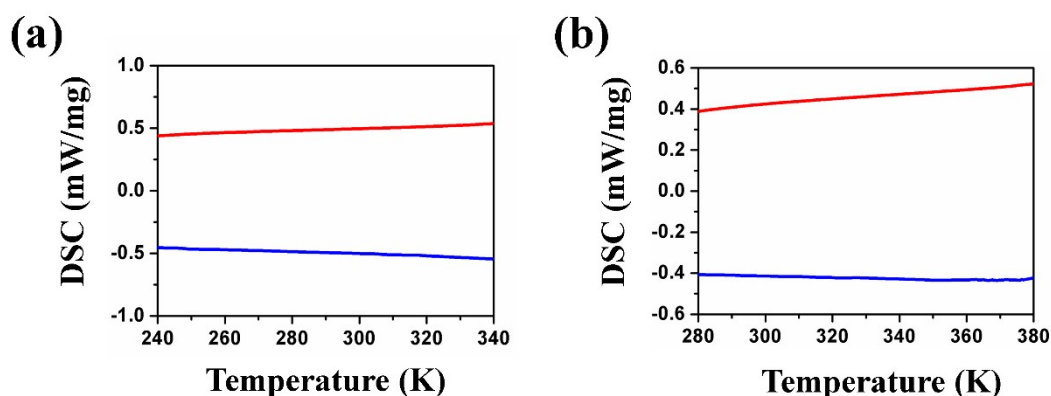


Fig. S1 DSC diagrams of compound 2 (a) and compound 3 (b).

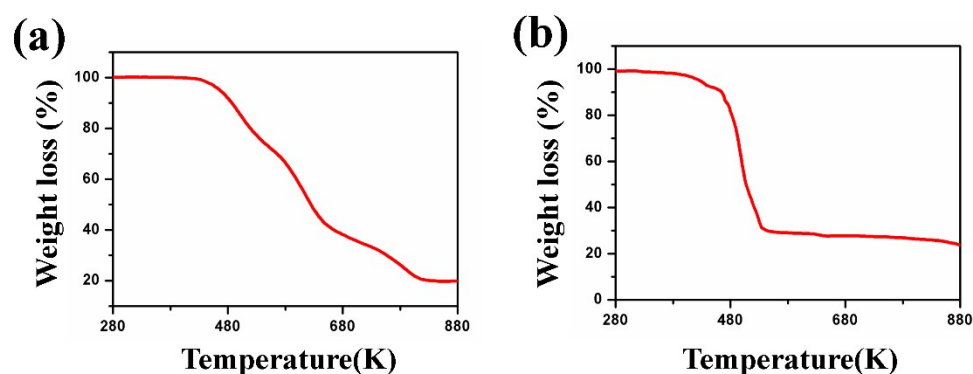


Fig. S2 Experimental TGA curves of compounds **1** (a) and **4** (b) in the temperature range from 280 K to 880 K

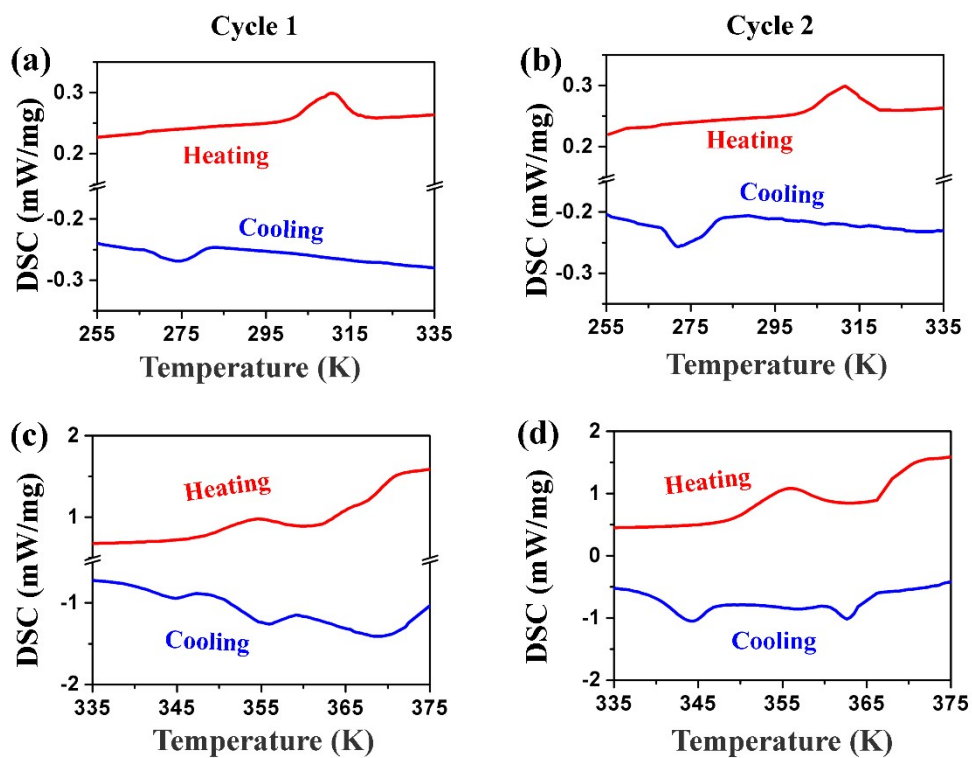


Fig. S3 DSC cycle plots of compound **1** (a), (b) and compound **4** (c), (d).

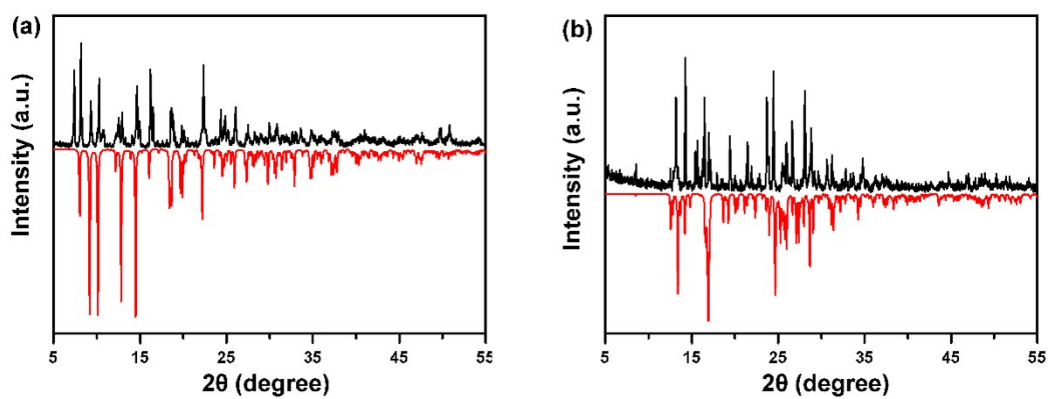


Fig. S4 Measured and simulated powder X-ray diffraction patterns of compounds **1** and **4** at 298 K.

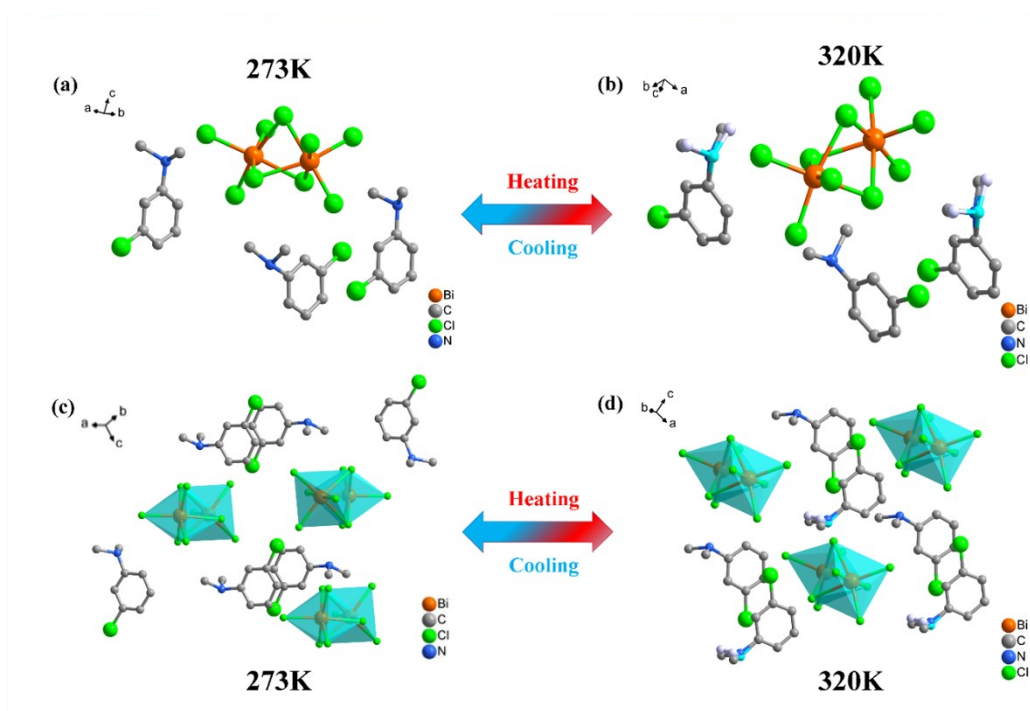


Fig. S5 (a) and (b) show the structural changes of the smallest asymmetric unit of compound **1** before and after heating. Stacking diagram of compound **1** at 273 K (c) and 320 K (d).

For compound **1**, at 273K, it crystallizes in the space group $P2(1)/m$, and the unit cell parameters are $a = 9.5873(11) \text{ \AA}$, $b = 22.042(3) \text{ \AA}$, $c = 9.7222(12) \text{ \AA}$, $\beta = 97.630(3)^\circ$, $V = 2377.61(17) \text{ \AA}^3$ and $Z = 2$. When heated to 320 K, the space group of compound **1** remain unchanged, with unit parameters $a = 9.6132(10) \text{ \AA}$, $b = 22.150(3) \text{ \AA}$, $c = 9.7574(12) \text{ \AA}$, $\beta = 97.628(3)^\circ$, $V = 2059.3(4) \text{ \AA}^3$ and $Z=2$ (Table S1). In addition, the zero-dimensional stacked structure of compound **1** containing organic ammonium and organic components was exhibited in Fig. S3. Although the cell parameters of compound **1** did not change significantly in the high temperature (HTP) stage compared with the low temperature stage (LTP), partial organic amine cations showed obvious disorder with the temperature rising. This process is clearly showed in Fig. S3.

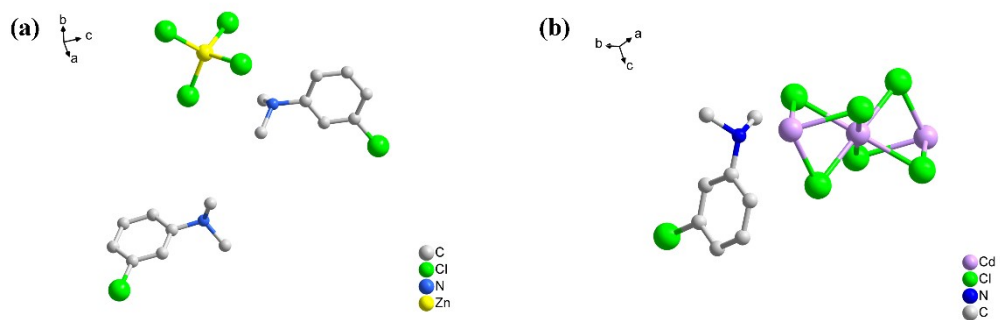


Fig. S6 (a) and (b) show the structural changes of the smallest asymmetric unit of compound **2** and compound **3** at 273K.

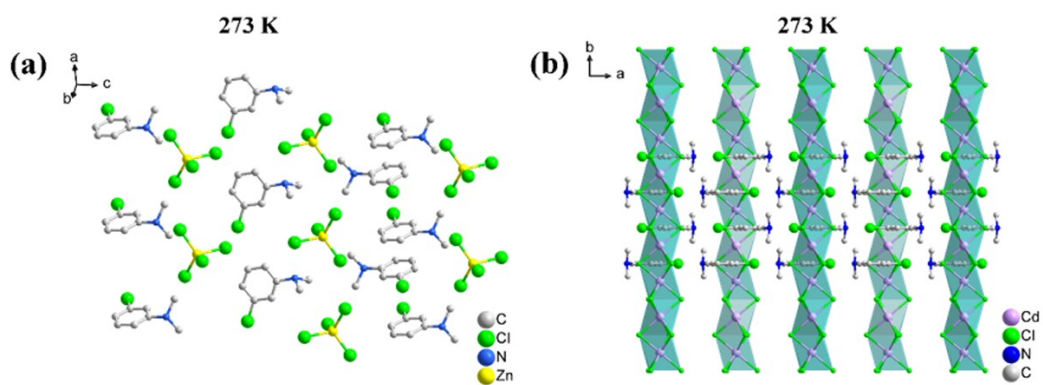


Fig. S7 Packaging diagram of compound **2** and compound **3** at 273 K.

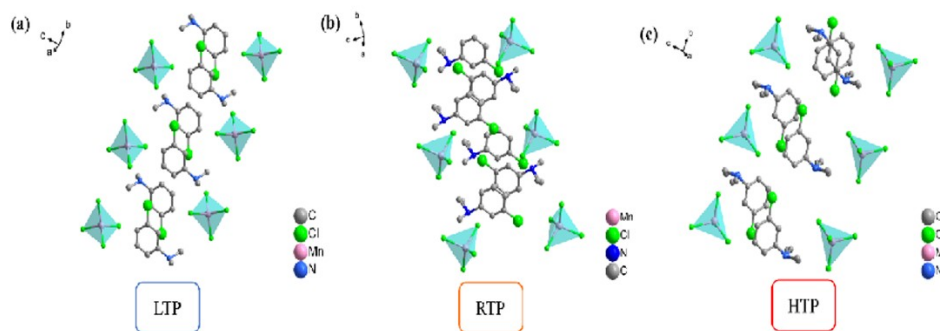


Fig. S8 Packaging diagram of compound **4** in LTP (a), RTP (b) and HTP (c).

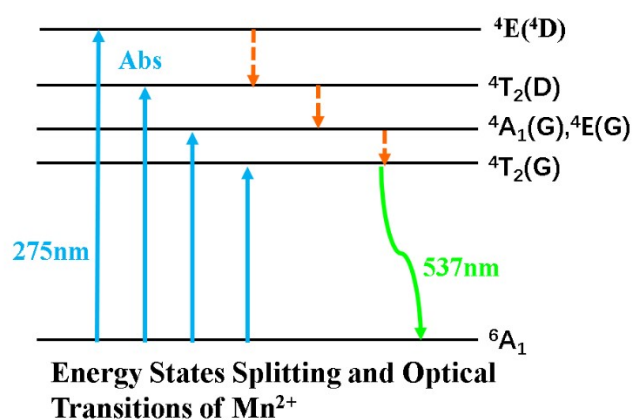


Fig. S9 The energy states splitting and optical transitions in tetrahedrally coordinated Mn²⁺ ion.

The energy level A_1 corresponds to the non-excited state (ground state) of compound **4**, while the green emission peak is 537 nm, which comes from the lowest ${}^4T_1 \rightarrow {}^6A_1$ transition. There are four main excitation peaks in the excitation spectrum of compound **4**, among which 275 nm belongs to a wide absorption band, while 355 nm, 430 nm and 450 nm are weak excitation bands, which belong to ${}^4T_2(D) \rightarrow {}^6A_1$, ${}^4A_1(G) \rightarrow {}^6A_1$ and ${}^4E(G) \rightarrow {}^6A_1$ and ${}^4T_2(G) \rightarrow {}^6A_1$ transition respectively.

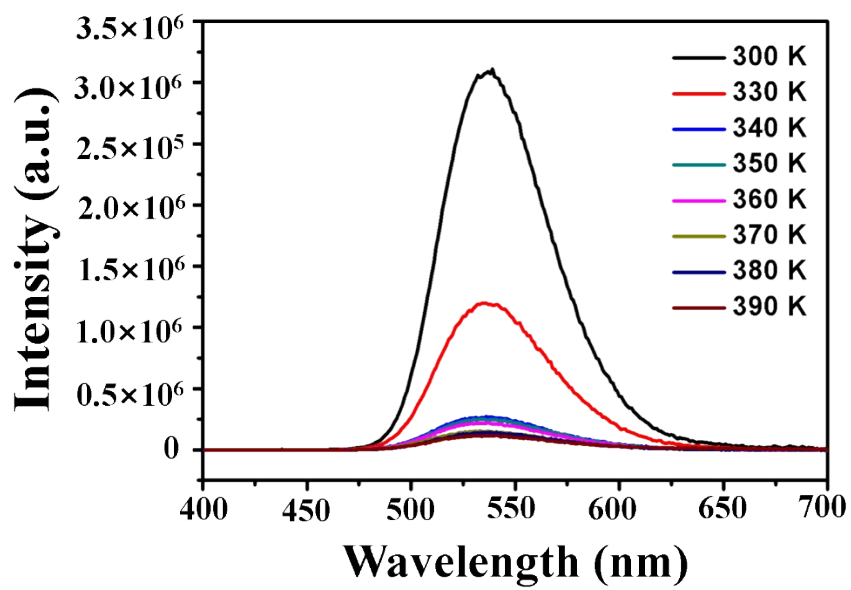


Fig. S10 Variable temperature fluorescence analysis plot of compound 4.

Table S1. Crystal data and structure refinements for compound **1** at 273 K and 320 K

	LTP (273 K)	HTP (320 K)
Empirical formula	C ₂₄ H ₃₄ Bi ₂ Cl ₁₂ N ₃	C ₂₄ H ₃₄ Bi ₂ Cl ₁₂ N ₃
Formula weight	1207.9	1207.9
Space group	<i>P</i> 21/ <i>m</i>	<i>P</i> 21/ <i>m</i>
Crystal system	Monoclinic	Monoclinic
a/ Å	9.5873 (11)	9.6132 (10)
b/ Å	22.042(3)	22.150 (3)
c/ Å	9.7222(12)	9.7574 (12)
β/°	97.630(3)	97.628(3)
Volume/ Å³	2036.3(4)	2059.3(4)
Z	2	2
F (000)	1138	1094
GOF	1.075	0.97
R1[<i>I</i>>2σ(<i>I</i>)]	0.065	0.038
wR2[<i>I</i>>2σ(<i>I</i>)]	0.152	0.100

Table S2. Crystal data and structure refinements for compound **2** at 273 K

	LTP (273 K)
Empirical formula	C ₁₆ H ₂₂ Cl ₆ N ₂ Zn
Formula weight	520.42
Space group	<i>P</i> $\bar{1}$
Crystal system	Triclinic
a/ Å	7.4644 (3)
b/ Å	7.7388 (3)
c/ Å	20.7344 (9)
β/°	97.630 (3)°
Volume/ Å³	1104.52 (8)
Z	2
F (000)	528
GOF	1.06
R1[<i>I</i>>2σ(<i>I</i>)]	0.041
wR2[<i>I</i>>2σ(<i>I</i>)]	0.099

Table S3. Crystal data and structure refinements for compound **3** at 273 K.

	LTP (273 K)
Empirical formula	C ₈ H ₁₁ CdCl ₄ N
Formula weight	375.38
Space group	<i>Pnma</i>
Crystal system	Orthorhombic
a/ Å	14.446 (2)
b/ Å	6.8496 (10)
c/ Å	12.429 (2)
β/°	97.630(3)
Volume/ Å³	1229.9 (3)
Z	4
F (000)	728
GOF	1.05
R1[I>2σ(I)]	0.037
wR2[I>2σ(I)]	0.089

Table S4. Crystal data and structure refinements for compound **4** at 273 K, 358K and 365K.

	LTP (273 K)	RTP (358 K)	HTP (365K)
Empirical formula	C ₁₆ H ₂₀ Cl ₆ MnN ₂	C ₁₆ H ₂₀ Cl ₆ MnN ₂	C ₁₆ H ₂₀ Cl ₆ MnN ₂
Formula weight	507.98	507.98	507.98
Space group	<i>P</i> $\bar{1}$	<i>P</i> $\bar{1}$	<i>P</i> $\bar{1}$
Crystal system	Triclinic	Triclinic	Triclinic
a/ Å	7.530	7.568 (4)	7.5849 (13)
b/ Å	7.699	8.088 (5)	7.7567(16)
c/ Å	20.946	20.838 (13)	21.082 (4)
β/°	94.56	95.451 (9)	94.901 (4)
Volume/ Å³	1133.2	1147.4 (12)	1154.5 (4)
Z	2	2	2
GOF	1.038	0.976	1.05
R1[I>2σ(I)]	0.0311	0.089	0.046
wR2[I>2σ(I)]	0.0799	0,248	0.133

Table S5. Selected bond lengths [Å] and bond angles for compound **1** at 273 K.

bond lengths [Å]		bond angles [Å]	
Bi1—Cl5	2.545 (2)	Cl5—Bi1—Cl3	92.50 (8)
Bi1—Cl1	2.564 (2)	Cl1—Bi1—Cl3	90.91 (9)
Bi1—Cl3	2.627 (2)	Cl5—Bi1—Cl6	92.85 (8)
Bi1—Cl6	2.862 (2)	Cl1—Bi1—Cl6	89.76 (8)
Bi1—Cl4	2.907 (2)	Cl3—Bi1—Cl6	174.56 (8)
Bi1—Cl2	2.952 (2)	Cl5—Bi1—Cl4	85.80 (8)
Cl2—Bi1i	2.952 (2)	Cl1—Bi1—Cl4	170.15 (7)
Cl4—Bi1i	2.907 (2)	Cl3—Bi1—Cl4	98.92 (8)
		Cl6—Bi1—Cl4	80.50 (7)
		Cl5—Bi1—Cl2	162.62 (7)
		Cl1—Bi1—Cl2	101.50 (8)
		Cl3—Bi1—Cl2	96.37 (8)
		Cl6—Bi1—Cl2	78.21 (7)
		Cl4—Bi1—Cl2	78.09 (7)

Table S6. Selected bond lengths [Å] and bond angles for compound **1** at 320 K.

bond lengths [Å]		bond angles [Å]	
Bi1—Cl6	2.5448 (14)	Cl6—Bi1—Cl4	93.18 (5)
Bi1—Cl4	2.5686 (15)	Cl6—Bi1—Cl3	92.57 (5)
Bi1—Cl3	2.6236 (14)	Cl4—Bi1—Cl3	91.09 (5)
Bi1—Cl5	2.8726 (12)	Cl6—Bi1—Cl5	93.18 (5)
Bi1—Cl1	2.9094 (13)	Cl4—Bi1—Cl5	89.67 (5)
Bi1—Cl2	2.9600 (14)	Cl3—Bi1—Cl5	174.14 (5)
Cl1—Bi1 ⁱ	2.9094 (13)	Cl6—Bi1—Cl1	86.02 (5)
Cl2—Bi1 ⁱ	2.9600 (14)	Cl4—Bi1—Cl1	169.93 (5)
Cl5—Bi1 ⁱ	2.8726 (12)	Cl3—Bi1—Cl1	98.97 (5)
		Cl5—Bi1—Cl1	80.36 (4)
		Cl6—Bi1—Cl2	163.14 (5)
		Cl4—Bi1—Cl2	101.22 (5)
		Cl3—Bi1—Cl2	95.83 (5)
		Cl5—Bi1—Cl2	78.33 (5)
		Cl1—Bi1—Cl2	78.26 (5)

Table S7. Selected bond lengths [Å] and bond angles for compound **2** at 273 K.

bond lengths [Å]		bond angles [Å]	
Zn1—Cl3	2.2382 (10)	Cl3—Zn1—Cl1	114.08 (4)
Zn1—Cl2	2.2661 (9)	Cl3—Zn1—Cl2	114.11 (4)
Zn1—Cl4	2.3104 (9)	Cl1—Zn1—Cl2	106.79 (3)
Cl1—Zn1	2.2488 (9)	Cl3—Zn1—Cl4	104.87 (4)
		Cl1—Zn1—Cl4	108.18 (3)
		Cl2—Zn1—Cl4	108.58 (3)

Table S8. Selected bond lengths [Å] and bond angles for compound **3** at 273 K.

bond lengths [Å]		bond angles [Å]	
Cd1—Cl2 ⁱ	2.6098 (6)	Cl2 ⁱ —Cd1—Cl2	180.00 (3)
Cd1—Cl2	2.6098 (6)	Cl2 ⁱ —Cd1—Cl4	97.42 (2)
Cd1—Cl4	2.6516 (7)	Cl2—Cd1—Cl4	82.58 (2)
Cd1—Cl4 ⁱ	2.6516 (7)	Cl2 ⁱ —Cd1—Cl4 ⁱ	82.58 (2)
Cd1—Cl3	2.6792 (6)	Cl2—Cd1—Cl4 ⁱ	97.42 (2)
Cd1—Cl3 ⁱ	2.6792 (6)	Cl4—Cd1—Cl4 ⁱ	180.0
Cd1—Cd1 ⁱⁱ	3.4248 (5)	Cl2 ⁱ —Cd1—Cl3	97.30 (2)
Cd1—Cd1 ⁱⁱⁱ	3.4248 (5)	Cl2—Cd1—Cl3	82.70 (2)
Cl2—Cd1 ⁱⁱⁱ	2.6098 (6)	Cl4—Cd1—Cl3	82.64 (2)
Cl3—Cd1 ⁱⁱⁱ	2.6792 (6)	Cl4 ⁱ —Cd1—Cl3	97.36 (2)
Cl4—Cd1 ⁱⁱⁱ	2.6516 (7)	Cl2 ⁱ —Cd1—Cl3 ⁱ	82.70 (2)
		Cl2—Cd1—Cl3 ⁱ	97.30 (2)
		Cl4—Cd1—Cl3 ⁱ	97.36 (2)
		Cl4 ⁱ —Cd1—Cl3 ⁱ	82.64 (2)
		Cl3—Cd1—Cl3 ⁱ	180.0
		Cl2 ⁱ —Cd1—Cd1 ⁱⁱ	48.993 (12)
		Cl2—Cd1—Cd1 ⁱⁱ	131.007 (12)
		Cl4—Cd1—Cd1 ⁱⁱ	130.226 (13)
		Cl4 ⁱ —Cd1—Cd1 ⁱⁱ	49.775 (13)
		Cl3—Cd1—Cd1 ⁱⁱ	129.728 (12)
		Cl3 ⁱ —Cd1—Cd1 ⁱⁱ	50.272 (12)
		Cl2 ⁱ —Cd1—Cd1 ⁱⁱⁱ	131.007 (12)
		Cl2—Cd1—Cd1 ⁱⁱⁱ	48.993 (12)
		Cl4—Cd1—Cd1 ⁱⁱⁱ	49.774 (13)
		Cl4 ⁱ —Cd1—Cd1 ⁱⁱⁱ	130.225 (13)
		Cl3—Cd1—Cd1 ⁱⁱⁱ	50.272 (12)
		Cl3 ⁱ —Cd1—Cd1 ⁱⁱⁱ	129.728 (12)
		Cd1 ⁱⁱ —Cd1—Cd1 ⁱⁱⁱ	180.0
		Cd1—Cl2—Cd1 ⁱⁱⁱ	82.01 (2)
		Cd1 ⁱⁱⁱ —Cl3—Cd1	79.46 (2)
		Cd1—Cl4—Cd1 ⁱⁱⁱ	80.45 (3)

Table S9. Selected bond lengths [Å] and bond angles for compound **4** at 273 K.

bond lengths [Å]		bond angles [Å]	
Cl1—Mn1	2.3628 (6)	Cl5—Mn1—Cl2	114.16 (3)
Cl2—Mn1	2.3390 (6)	Cl5—Mn1—Cl1	113.70 (3)
Cl4—Mn1	2.3973 (6)	Cl2—Mn1—Cl1	106.65 (2)
Cl5—Mn1	2.3338 (6)	Cl5—Mn1—Cl4	104.41 (3)
		Cl2—Mn1—Cl4	108.31 (2)
		Cl1—Mn1—Cl4	109.47 (2)

Table S10. Selected bond lengths [Å] and bond angles for compound **4** at 358 K.

bond lengths [Å]		bond angles [Å]	
Mn1—Cl1	2.332 (3)	Cl1—Mn1—Cl3	118.90 (12)
Mn1—Cl3	2.347 (3)	Cl1—Mn1—Cl4	116.12 (12)
Mn1—Cl4	2.347 (3)	Cl3—Mn1—Cl4	104.23 (11)
Mn1—Cl2	2.424 (3)	Cl1—Mn1—Cl2	103.29 (12)
		Cl3—Mn1—Cl2	108.30 (11)
		Cl4—Mn1—Cl2	105.04 (11)

Table S11. Selected bond lengths [Å] and bond angles for compound **4** at 365 K.

bond lengths [Å]		bond angles [Å]	
Mn1—Cl6	2.3277 (12)	Cl6—Mn1—Cl4	113.79 (5)
Mn1—Cl4	2.3386 (11)	Cl6—Mn1—Cl5	114.21 (5)
Mn1—Cl5	2.3589 (10)	Cl4—Mn1—Cl5	106.44 (4)
Mn1—Cl3	2.3916 (10)	Cl6—Mn1—Cl3	104.38 (5)
		Cl4—Mn1—Cl3	108.66 (4)
		Cl5—Mn1—Cl3	109.22 (4)

Table S12. Hinside-Cloutside surface area, mean di and mean de of different amine in **1** and **4**.

Compound	Temperature	Hinside-Cloutside surface area		Mean di	Mean de
1	273 K	Cation 1	39.5%	1.6917	1.9380
		Cation2	43.3%	1.7691	2.0231
	320K	Cation1	38.8%	1.7013	1.9266
		Cation2	42.3%	1.7367	2.0197
2	273 K	Cation1	33.2%	1.6660	1.9042
		Cation2	32.6%	1.6622	1.8729
	365K	Cation1	31.9%	1.6438	1.8650
		Cation2	31.5%	1.6499	1.8906

Reference

1. Turner, M. J.; McKinnon, J. J.; Wolff, S. K.; Grimwood, D. J.; Spackman, P. R.; Jayatilaka, D.; Spackman, M. A. CrystalExplorer17; University of Western Australia, 2017, <http://hirshfeldsurface.net>